OPTIMUM SYNTHESIS OF PATH GENERATING ADJUSTABLE MECHANISMS WITH IMPROVED SLOPE CONTINUITY OF THE CONTROL PARAMETER

Hrishikesh Y. Raste[1], Ameya P. Apte[2], Gunesh R. Gogate[3]

[1] *PARI Robotics, Pune, India.*
[2] *Department of Mechanical Engineering, Purdue University, West Lafayette, USA.*
[3] *Neha Engineering Solutions, Pune, India.*
e-mail: grgogate@gmail.com

Received July 2012, Accepted July 2013
No. 12-CSME-85, E.I.C. Accession Number 3405

ABSTRACT

Adjustable mechanisms have been studied in literature for path and function generation. In this paper, a path generating four-bar mechanism with an alternate single parameter adjustment is proposed and optimally synthesized, using the method of Differential Evolution. Two new approaches are developed, aimed at improving the slope continuity characteristic of the control parameter. Optimum synthesis results are obtained using the proposed approaches. The results show that the proposed approaches lead to improved slope continuity characteristics of the control parameter.

Keywords: adjustable mechanisms; path generation; optimum synthesis; differential evolution.

SYNTHÈSE OPTIMALE DU MÉCANISME RÈGLABLE DE GÉNÉRATION DE TRAJECTOIRE AVEC UNE CONTINUITÉ AMÉLIORÉE DE LA PENTE DU PARAMÈTRE DE CONTRÔLE

RÉSUME

Une revue de la littérature montre que les mécanismes réglables pour la génération de trajectoire et de fonction ont déjà été étudiés. . Dans cet article, un mécanisme à quatre barres avec un ajustement de paramètre alternatif unique est proposé, et la synthétisation optimale est faite en utilisant la méthode de l'évolution différentielle. Deux nouvelles approches sont développées, visant à améliorer la caractéristique de continuité de la pente du paramètre de contrôle. Les résultats de la synthèse optimale sont obtenus en appliquant les approches proposées. Ces résultats indiquent que les approches proposées mènent aux caractéristiques de continuité de la pente du paramètre de contrôle.

Mots-clés : mécanismes réglables ; génération de trajectoire ; synthèse optimale ; évolution différentielle.

1. INTRODUCTION

Function, Path and Motion Generation are the three broad categories of kinematic tasks for which mechanisms are widely used in practice. The most commonly used mechanism is the four-bar mechanism, as it is one of the simplest mechanisms, and is relatively easy to synthesize. As far as exact synthesis is concerned, however, the four-bar mechanism has limitations in terms of the number of precision points or poses that can be satisfied, due to the small number of design parameters it has. Researchers have proposed the use of five-bar mechanisms [1–4], and of adjustable mechanisms [5–9], to overcome this problem.

Synthesis of a geared five-bar path generating mechanism using the continuation method was presented in [1], wherein the gear ratio could be varied. Optimum synthesis of Grashof geared five-bar mechanisms was presented in [2], wherein the optimization was carried out using a quasi-Newton method. Optimum synthesis of five-bar linkages with non-circular gearing between the two input links was presented for exact path generation [3], using a genetic algorithm. The path generation capability of five-bar slider-crank parallel manipulators was investigated in [4]. They were classified into two types, and the capability of each type to generate a singularity-free path was analyzed.

Adjustable linkages with discrete or continuous adjustment have been proposed by many, especially for function and path generation applications. Use of a cam-link mechanism was proposed in [5] to generate the desired path precisely, in which a fixed cam was used to adjust the length of the side link of the four-bar linkage. Slider-crank linkages with continuous adjustment of the slider offset were synthesized in [6], to precisely generate desired paths. Precise generation of continuous paths was achieved by using hybrid cam-linkage mechanisms in [7]. The relative locations of the joints were adjusted by using cams. Optimum synthesis of a function generating adjustable four-bar mechanism, in which the position of the output fixed pivot was continuously adjusted by using an additional revolute link, was presented in [8]. Synthesis of an adjustable four-bar mechanism for path generation was presented in [9]. A slider was added to the four-bar, which would be used to continuously adjust the position of the output fixed pivot. Optimization was carried out using a genetic algorithm.

As can be seen from the discussion presented above, continuous 1-parameter adjustment of a four-bar mechanism has been proposed by Zhou for function [8] and path generation [9], wherein a link is added to the four-bar, essentially converting it into a five-link mechanism with degree of freedom equal to 2. The resulting mechanism is then synthesized as an adjustable four-bar mechanism, since the total variation of the 'control or adjustment parameter' is kept as small as possible. The other input parameter of the adjustable mechanism is continuously changed, making it the 'input variable' or 'input displacement'. No gearing is used to couple the two input links. This paper extends the work by Zhou [9] in two ways. Firstly, it presents optimum synthesis of an adjustable 4-bar mechanism with an alternate one-parameter adjustment, for path generation. Secondly, it presents two new approaches to tackle the problem of slope discontinuity of the control parameter, reported in [9].

The organization of the paper is as follows. The proposed adjustable mechanism and its position analysis are presented in Section 2. In Section 3, the formulation of the optimization problem is presented. The error functions used, and the proposed approaches aimed at improving the slope continuity of the control parameter are presented in Section 4. In Section 5, constraints imposed in the

optimization process are presented. The Differential Evolution algorithm is presented in Section 6. Scheme of path discretization and results are presented in Section 7, followed by conclusions in Section 8.

2. THE PROPOSED ADJUSTABLE MECHANISM

Fig. 1 shows the proposed adjustable mechanism $ABCDE$, which consists of a four-bar $ABCD$, and an added link ED. In this work, the specified path is assumed to be a closed path and is discretized by choosing points $M_i(X_i, Y_i), i = 1, 2, \ldots, n,$ along the path. Links AB and ED respectively make $\angle\theta$ and $\angle\varphi$ with the *X*-axis, which are measured positive anticlockwise. Let $\angle BCD = \eta$ and $\angle CDE = \mu$. Link ED is to be used as a controlling link, to adjust the position of the 'fixed pivot' of the four-bar, 'D', along the circle with 'E' as the center and ED as the radius. This adjustment is to be made in such a way that a coupler point F of the four-bar would exactly pass through the chosen points on the specified path. Towards this, inverse position analysis of the proposed adjustable mechanism is presented in this section, assuming that the coupler point F coincides with a chosen path point. 'θ' and 'φ' represent the 'input variable' (or displacement) and the 'control parameter' respectively. This choice of control parameter has been used by Zhou [8] for function generation, and may be preferred to that presented in [9], since it makes use of an additional revolute link, instead of a sliding link.

With reference to Fig. 1, the following link dimensions and angles are noted.

$$AB = L_1,\ BC = L_2,\ CD = L_3,\ DE = L_4,\ BF = L_5,\ \angle CBF = \delta.$$

The vector of design variables, $\boldsymbol{X}$, is as follows.

$$\boldsymbol{X} = [X_A, Y_A, X_E, Y_E, L_2, L_3, L_4, \delta].$$

Variables L_1 and L_5, which are not included in $\boldsymbol{X}$, are calculated using Eqs. (1–2).

$$L_1 + L_5 = d_{max} \tag{1}$$

$$|L_1 - L_5| = d_{min} \tag{2}$$

Here, $d_{max} = max\{dist(AM_i)\}$ and $d_{min} = min\{dist(AM_i)\}$. These equations follow from the requirement that the input AB should be a crank, and the assumption that the path to be generated is a closed curve [9].

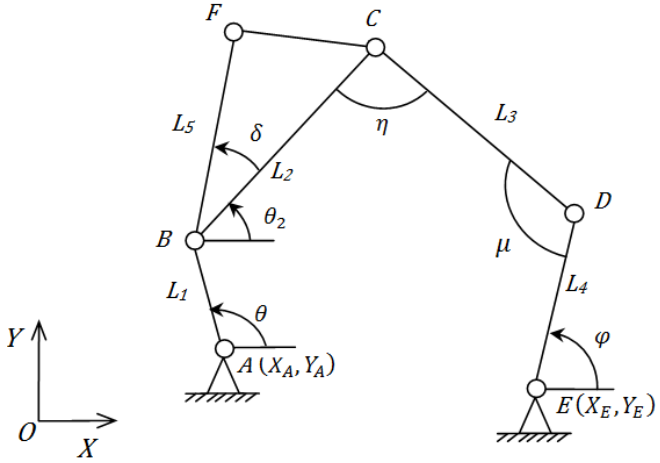

Fig. 1. The proposed adjustable four-bar mechanism.

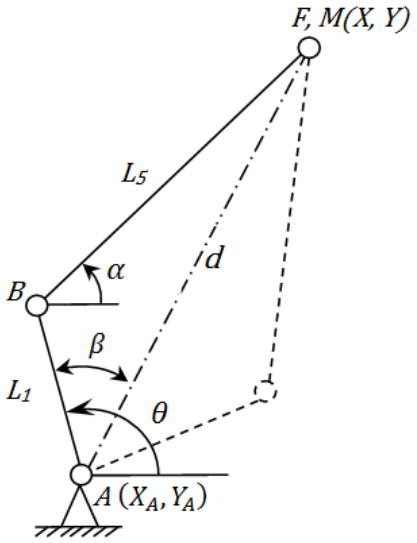

Fig. 2. Dyad *ABF*.

Fig. 2 shows the two possible configurations of the input dyad ABF, when F coincides with a path point $M_i\left(X_i, Y_i\right)$, denoted by $M(X,Y)$ for convenience. The following expressions are obtained from Fig. 2.

$$d = \sqrt{\left(X_A - X\right)^2 + \left(Y_A - Y\right)^2} \tag{3}$$

$$\beta = \cos^{-1}\left(\frac{L_1^{\,2} + d^2 - L_5^2}{2L_1 d}\right) \tag{4}$$

$$\theta = Atan2\left[\left(Y - Y_A\right), \left(X - X_A\right)\right] \pm \beta \tag{5}$$

'$Atan2$' is the two-argument inverse tangent function, which returns the value of the angle in the correct quadrant.

Coordinates of B:

$$X_B = X_A + L_1 \cos\theta \tag{6}$$

$$Y_B = Y_A + L_1 \sin\theta \tag{7}$$

Angle α:

$$\alpha = Atan2\left[\left(Y - Y_B\right),\left(X - X_B\right)\right] \tag{8}$$

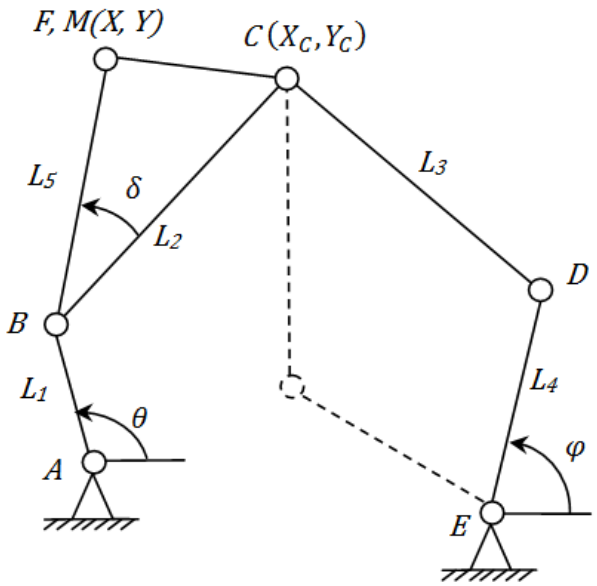

Fig. 3. Configurations of the adjustable mechanism for a chosen configuration of dyad *ABF*.

One of the two possible configurations of the dyad ABF must be chosen while carrying out the optimization, as discussed in Section 7. From Figs. 1–3, it is seen that when the coupler point F coincides with a path point M, C occupies a position $\left(X_C, Y_C\right)$ given by,

$$X_C = X_B + L_2 \cos\theta_2 \tag{9}$$

$$Y_C = Y_B + L_2 \sin\theta_2 \tag{10}$$

where $\theta_2 = \alpha - \delta$ is the angle made by BC with *X*-axis, as shown in Fig. 1. Fig. 4 shows the two possible configurations of dyad EDC, for which the following equations are obtained. Here $d' = dist(EC)$.

$$d' = \sqrt{(X_E - X_C)^2 + (Y_E - Y_C)^2} \tag{11}$$

$$\gamma = \cos^{-1}\left(\frac{L_4^2 + d'^2 - L_3^2}{2L_4 d'}\right) \tag{12}$$

$$\varphi = Atan2\left[\left(Y_C - Y_E\right),\left(X_C - X_E\right)\right] \pm \gamma \tag{13}$$

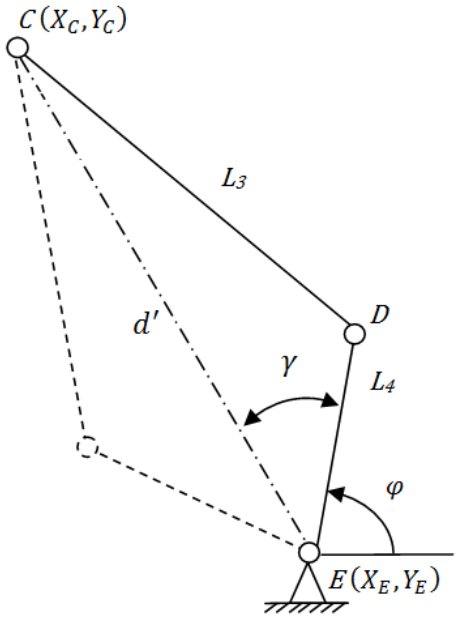

Fig. 4. Dyad *EDC*.

Coordinates of *D*:

$$X_D = X_E + L_4 \cos\varphi \tag{14}$$

$$Y_D = Y_E + L_4 \sin\varphi \tag{15}$$

$$BD = \sqrt{(X_B - X_D)^2 + (Y_B - Y_D)^2} \tag{16}$$

$$CE = \sqrt{(X_C - X_E)^2 + (Y_C - Y_E)^2} \tag{17}$$

Angles η and μ:

$$\eta = \cos^{-1}\left(\frac{L_2^2 + L_3^2 - BD^2}{2L_2L_3}\right) \tag{18}$$

$$\mu = \cos^{-1}\left(\frac{L_3^2 + L_4^2 - CE^2}{2L_3L_4}\right) \tag{19}$$

Eqs. (1–19) represent the complete inverse position analysis of the adjustable mechanism, which is used to ensure that the specified path points are exactly traced by 'F', and also to calculate the error functions and to check the constraints, as explained later in Sections 4 and 5. Details regarding the choice of the configuration of dyad EDC are presented in Section 7.

3. THE OPTIMIZATION PROBLEM

An objective function, denoted as OF, is that function of the design vector $\boldsymbol{X}$, which is sought to be optimized. An approach that is commonly used in evolutionary algorithms is to define OF as the sum of an 'error function' and 'penalties' associated with the violation of the imposed constraints [10,11,14], as follows.

$$OF(\boldsymbol{X}) = EF(\boldsymbol{X}) + \sum k_i h_i(\boldsymbol{X}) \tag{20}$$

where $EF(\boldsymbol{X})$ represents the error function and k_i are the constraint penalties. $h_i(\boldsymbol{X})$ is a function of $\boldsymbol{X}$ which attains a value '1', whenever $\boldsymbol{X}$ violates the i^{th} constraint, and a value '0' otherwise.

The optimization problem can now be formulated as follows.

Minimize OF subject to $x_i \in [LL_i, UL_i] \quad \forall x_i \in \boldsymbol{X}$, where LL_i and UL_i are the lower and upper limits specified for variable x_i.

4. ERROR FUCNTIONS

In the following, subscript 'i' is used to denote the value attained by a variable, when point F coincides with the path point M_i. As the coupler point F of a particular adjustable mechanism traces the specified path, 'θ' varies through 360^0, whereas 'φ' varies within a range $[\varphi_{min}, \varphi_{max}]$. There can be many adjustable mechanisms that can trace the specified path points exactly. It is in general desirable that the net adjustment is as small as possible. Keeping this in mind, an error function $EF1$ is defined as follows.

$$EF1 = \varphi_{max} - \varphi_{min} = \Delta\varphi \tag{21}$$

$EF1$, defined as in Eq. (21), is same as that used by Zhou [8–9]. If the specified path has slope discontinuities (e. g., a polygonal path), then the control parameter may also exhibit slope discontinuities, with respect to the input displacement as the independent variable [9]. This should be avoided to the extent possible, since accurately adjusting the control parameter would not be possible in the presence of slope discontinuities, resulting in the coupler point not exactly passing through the path points. It was suggested in [9] that this problem could be tackled by modifying the specified path itself. However, this approach would defeat the basic purpose behind using an adjustable mechanism.

In this work, this problem is tackled using two new approaches, which utilize a measure of slope discontinuity defined as follows.

$$\text{Maximum Slope Discontinuity } (MSD) = max \left| \frac{\Delta\varphi_{i+1}}{\Delta\theta_{i+1}} - \frac{\Delta\varphi_i}{\Delta\theta_i} \right| \tag{22}$$

'*MSD*' represents an approximation to the maximum change in the derivative of 'φ' with respect to 'θ' between a pair of adjacent path points. In Eq. (22), $\Delta\varphi_i = \varphi_{i+1} - \varphi_i$ and $\Delta\theta_i = \theta_{i+1} - \theta_i$. For $i = n$, the subscript '$n+1$'needs to be replaced by '1'.

The first approach is based on using $EF1$ as the error function, while imposing a constraint on the maximum value of *MSD*, during the process of optimization. This would result in restricting the

maximum value of *MSD*, while minimizing $\Delta\varphi$. The details of the constraint imposed on *MSD* are presented in Section 5.

The second approach is based on the minimization of an objective function based on a new error function $EF2$, which is defined as

$$EF2=\left(\varphi_{max}-\varphi_{min}\right)+w.max\left|\frac{\Delta\varphi_{i+1}}{\Delta\theta_{i+1}}-\frac{\Delta\varphi_i}{\Delta\theta_i}\right|=\Delta\varphi+w.MSD \tag{23}$$

where 'w' is the weight attached to MSD. This definition of $EF2$ is aimed at minimizing a weighted sum of the 'net adjustment' and the discontinuity in the derivative of 'φ' with respect to 'θ', so as to provide an indirect control over MSD.

5. CONSTRAINTS

The following constraints are imposed during the optimization process.

Constraint 1: Imposition of this constraint ensures that the synthesized mechanism is free from 'order defect', so that the path points are traced in the correct order, as link AB is rotated continuously. Towards this, either Eq. (24) or Eq. (25) must be satisfied.

$$\theta_i < \theta_{i+1} \qquad \text{for all } i \tag{24}$$

$$\theta_i > \theta_{i+1} \qquad \text{for all } i \tag{25}$$

Constraint 2: It must be possible to assemble dyad EDC in all positions of dyad ABF, for which L_3 and L_4 must satisfy Eqs. (26–27).

$$L_3 + L_4 \geq d'_{max} \tag{26}$$

$$\left|L_3 - L_4\right| \leq d'_{min} \tag{27}$$

Here, $d'_{max}=max\{dist\ (EC_i)\}$ and $d'_{min}=min\{dist\ (EC_i)\}$, as shown in Fig. 4. It should be noted that satisfaction of constraint 2, together with the fact that Eqs. (1–2) are used to calculate L_1 and L_5, ensures that the input link AB would be a crank, so that the synthesized mechanism can be operated by a rotary actuator.

Constraint 3: It is required that angle μ (Fig. 1) satisfies Eq. (28), in order to avoid near-alignment of links ED and DC.

$$0^0 < \mu_{min} \leq \mu_i \leq \mu_{max} < 180^0 \tag{28}$$

The limiting values of μ are selected to be $\mu_{min}=20^0$ and $\mu_{max}=160^0$. This also ensures that the dyad EDC would always remain in the same configuration.

Constraint 4: A constraint is similarly imposed on η, as follows.

$$0^0 < \eta_{min} \leq \eta_i \leq \eta_{max} < 180^0 \tag{29}$$

The limiting values of η are selected to be $\eta_{min} = 20^0$ and $\eta_{max} = 160^0$.

It should be noted that constraints 3 and 4 are imposed to ensure effective motion and force transmission.

Constraint 5: A constraint is imposed on the ratio of the longest link length to the shortest link length, so that the synthesized mechanism is proportionate.

$$\frac{L_{max}}{L_{min}} \leq r_1 \tag{30}$$

In this work, 'r_1' is assigned a value of 6.0.

Constraint 6: A constraint is imposed on the maximum value of MSD, while generating the '$EF1$ with constraint on MSD' results.

$$MSD \leq r_2 \tag{31}$$

Whenever a constraint is violated, a penalty is added to the value of the objective function, as indicated by Eq. (20).

Apart from these six constraints, it is required that the design variables lie within ranges, which are specified while initializing the population of mechanisms. If the value of any design variable goes beyond its specified range during the process of optimization, then it is re-set to that limit value, which is closer to the current value of the variable.

6. OPTIMIZATION ALGORITHM

Price, Storn and Lampinen [13] developed the method of 'Differential Evolution' (DE), which has been used for optimum synthesis of mechanisms [11,14]. From among the various DE strategies proposed in [13], the following strategy is used in this work.

The first step is to randomly initialize the population, after which mutation and crossover are carried out for $i = 1$ to N_p, where N_p is the population size. In mutation, the best vector from the current generation, $\boldsymbol{X_{best}}$, is perturbed by using a weighted differential of a randomly chosen pair of vectors $(\boldsymbol{X_a}, \boldsymbol{X_b})$ from the current generation, and a scale factor f_s, to generate a new mutant vector, $\boldsymbol{X_{ci}}$. This is mathematically represented as $\boldsymbol{X_{ci}} = \boldsymbol{X_{best}} + f_s * (\boldsymbol{X_a} - \boldsymbol{X_b})$. The vectors $\boldsymbol{X_a}$ and $\boldsymbol{X_b}$ are chosen by 'Random offset selection', so that they are never the same. In the next step, the i^{th} vector from the current population $\boldsymbol{X_i}$, is used for crossover with the i^{th} mutant $\boldsymbol{X_{c_i}}$, to produce a trial vector $\boldsymbol{X_{t_i}}$. The type of crossover used is called 'uniform crossover' or 'discrete recombination' [13]. The fraction of parameter values that are copied from the vector $\boldsymbol{X_{c_i}}$ to $\boldsymbol{X_{t_i}}$ is controlled by the crossover probability C_r, which lies in the range $[0, 1]$. Mathematically, the j^{th} component of $\boldsymbol{X_{t_i}}$ is assigned as

$$X_{t_{i,j}} = \begin{cases} X_{c_{i,j}}, if\ (rand)_j \le C_r\ or\ j = k \\ \\ X_{i,j}, otherwise \end{cases}$$

where $j = 1, \ldots, n$, ' n ' being the number of components of the design vector. ' k ' is an integer randomly chosen for each ' j ', from the integers [1, 2, …, n], whereas ' $(rand)_j$ ' is a number randomly generated in the range [0 1]. Both ' $(rand)_j$ ' and ' k ' are generated using the 'rand' command available in MATLAB'. The objective function values for the vectors $\boldsymbol{X}_{t_i}$ and $\boldsymbol{X}_i$ are compared, and the one with a lower value survives to become a member of the next generation.

A code was written in MATLAB, to implement the DE algorithm. The following convergence criteria are used.

i. Maximum number of generations $N_{g,max}$, for which the algorithm should run, is specified.

ii. The algorithm would terminate if for a specified number of successive generations (N_g), the change in the objective function value is less than or equal to a specified tolerance value (OF_{tol}) .

Trial runs were carried out to decide the appropriate values of the parameters associated with the algorithm, which are given below.

$$N_p = 100,\ N_{g,max} = 300,\ N_g = 50,\ OF_{tol} = 10^{-5},\ C_r = 0.8,\ f_s = 0.9.$$

Penalties:

k_i = 250 for i = 1 to 6.

20 runs of the DE algorithm were taken for each case, and the best solutions were used for comparative analysis.

7. RESULTS AND DISCUSSION

In this section, the scheme used to discretize the path is presented, followed by the results for an example problem.

A specified path has to be discretized, by selecting suitable path points on it. A sufficiently large number of path points must be selected so that the path is traced accurately. On the other hand, the number of path points should not be excessively large, since the computational time would increase with the number of path points.

An obvious scheme to discretize the specified path would be to select equidistant path points, i.e., path points with uniform spacing. However, for a path having slope discontinuities, it is desirable that a finer discretization is achieved in the vicinity of slope discontinuities, and also that the points of slope discontinuity are necessarily selected as path points. This would ensure that the path is better

approximated in the vicinity of the slope discontinuities, and that the 'maximum slope discontinuity' term is accurately computed. Towards this, an alternative discretization scheme is considered in this work, as follows.

'Chebyshev' spacing of accuracy points is commonly used in synthesis of mechanisms, which results in closely spaced accuracy points near the endpoints of the variable interval. However, the endpoints of the interval are not selected as accuracy points, due to certain mathematical properties of the underlying Chebyshev polynomials. The alternate scheme used here discretizes a slope-continuous segment of the path by using Chebyshev spacing for internal path points, and by selecting the end points of the segment (at which the slope is discontinuous) as additional path points. This scheme is hereafter referred to as the 'modified Chebyshev spacing'.

'N' points with Chebyshev spacing, within an interval $[x_i,\ x_f]$ of a variable 'x', are given by the following formula [12].

$$x(j) = x_i + \frac{1}{2}(x_f - x_i)\left[1 - \cos\left(\frac{\pi(2j-1)}{2N}\right)\right], \qquad j = 1,2,\ldots,N \tag{32}$$

The following steps are executed to discretize each 'slope continuous' portion of a specified path, using the proposed scheme.

a. N_s, the total number of segments within the concerned 'slope continuous' portion of the path, is specified.
b. The two end points are selected as the path points numbered as '1' and 'N_s+1'.
c. The (N_s-1) number of intermediate path points (points '2' to N_s) are selected using Eq. (32), with $N = N_s - 1$. The distance along the path, from any of the two end points, plays the role of the variable 'x'.

The 'modified Chebyshev' scheme of path discretization is illustrated in Fig. 5, for a slope-continuous portion P_iP_{i+1} of a path, for $N_s = 6$.

Problem:

The specified path is a rectangle shown in Fig. 6, having its four corner points at $P1(1.0, 0.25), P2(-1.0, 0.25), P3(-1.0, -0.25)$ and $P4(1.0, -0.25)$. The slope continuous segments of the path are: $P1P2, P2P3, P3P4$ and $P4P1$. The ranges for the design variables are specified as follows.

X_A, Y_A, X_E, Y_E : [–4.0, 4.0]; L_2, L_3, L_4 : [0.0, 5.0]; δ : [0, 2π].

For a candidate mechanism, L_1 and L_5 are evaluated using Eqs. (1–2). Out of the two resulting pairs of values of L_1 and L_5, that pair is selected which satisfies the condition $L_1 \le L_5$. In this work, two separate programs were written, one for each of the two configurations of the dyad ABF. These two programs are run separately leading to two optimum solutions, the one with the smaller value of the objective function being treated as the optimum mechanism. Both configurations of dyad EDC are retained in the synthesis process, and evaluation of the objective function is carried out for the two mechanisms consisting of the chosen dyad ABF and each of the two configurations of dyad EDC, using Eq. (20). The mechanism with the larger value of the objective function is discarded and the one with the smaller value is retained in the current population of mechanisms.

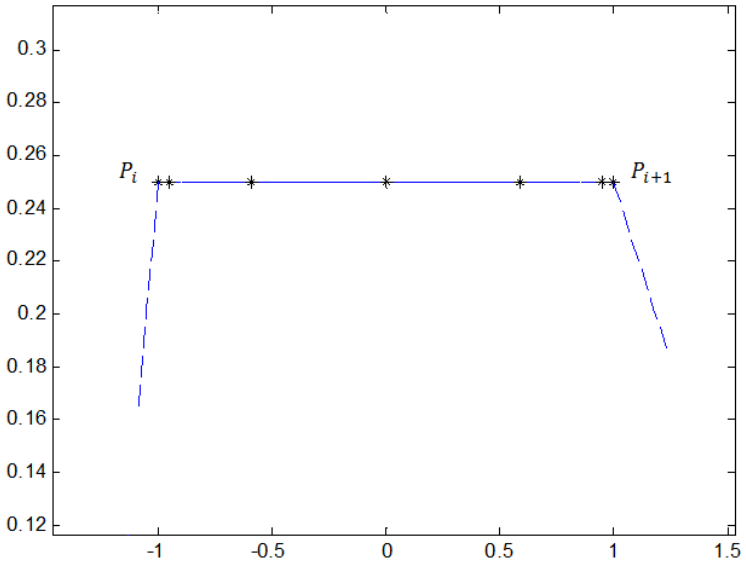

Fig. 5. Modified Chebyshev spacing of path points.

For the rectangular path shown in Fig. 6, results were initially obtained for the error function $EF1$, using 60 and 80 path points with uniform spacing. Similarly, results were obtained for 60 (10 segments along the shorter side, 20 segments along the longer side) and 80 (14 segments along the shorter side, 26 segments along the longer side) path points with modified Chebyshev spacing. The minimized values of the objective function were found to be almost equal for the two types of spacing, for the same number of path points. Control parameter φ was plotted against the input variable θ, for each case. It was found that 60 path points were insufficient, as the plots of φ versus θ showed many straight line portions. The plot for 80 points with uniform spacing also showed a few straight line portions, indicating that 80 points with uniform spacing were not sufficient. The plot for 80 points with modified Chebyshev spacing showed no straight line portions, indicating that 80 points with modified Chebyshev spacing were sufficient to discretize the specified path. Optimization results obtained using a higher number of path points (100 path points, 18 segments along the shorter side, 32 segments along the longer side) showed no significant change in the optimum value of the objective function. All the results presented are, therefore, for 80 path points with modified Chebyshev spacing.

Results are obtained for the following cases.

i. ‘$EF1$’ results: Error Function $EF1$, constraint 6 is not imposed.

ii. ‘$EF1$ with constraint on MSD’ results: Error Function $EF1$, constraint 6 is imposed.

iii. ‘$EF2$’ results: Error Function $EF2$, constraint 6 is not imposed.

The optimized mechanisms are presented in Tables 1 and 2, together with the values of the objective function (OF), the total change in the control parameter ($\Delta\varphi$) and the ‘maximum slope discontinuity’ term (MSD).

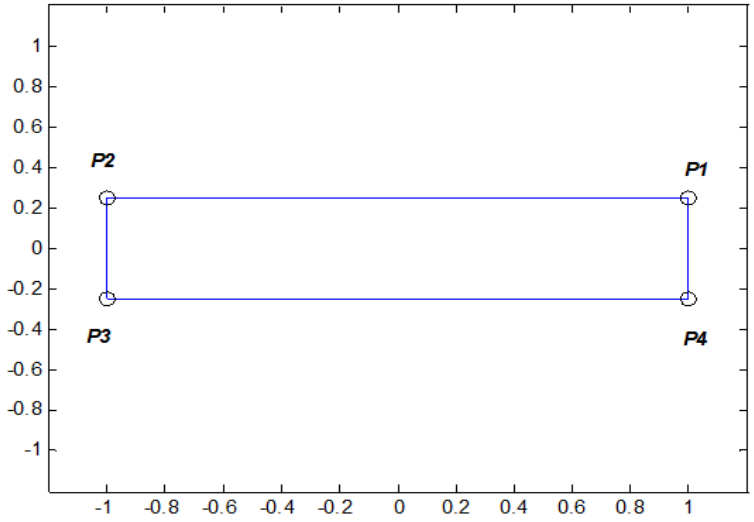

Fig. 6. Specified path.

Table 1. Optimized '$\boldsymbol{EF1}$' and '$\boldsymbol{EF1}$ with constraint on *MSD*' mechanisms.

Design Variables	**EF1**		**EF1 with constraint on MSD**	
	(1)	**(2)**	**(3)**	**(4)**
		$r_2 = 0.3$	$r_2 = 0.2$	$r_2 = 0.1$
X_A	2.1759	-3.4658	-2.5721	3.3954
Y_A	3.2071	-3.2313	-2.8193	3.7605
X_E	4.0000	-4.0000	2.2026	4.0000
Y_E	4.0000	-4.0000	-1.0495	-1.3037
L_2	2.8072	3.9930	1.5252	1.7156
L_3	3.9909	4.9954	3.0396	2.7873
L_4	4.5363	4.3886	4.2775	5.0000
ρ	349.0402^0	73.5048^0	0.0^0	53.6919^0
L_1	0.7561	0.8968	0.8488	0.8501
L_5	3.9384	4.7657	3.8609	5.1000
OF	0.0501	0.0935	0.1773	0.2839
$\Delta\varphi(rad)$	0.0501	0.0935	0.1773	0.2839
MSD	**0.4769**	**0.3**	**0.1999**	**0.1**

Mechanism 1 (Table 1) represents the $EF1$ mechanism, for which MSD is seen to be 0.4769, which is calculated from its definition. The‘ $EF1$ with constraint on MSD ’ results were generated for $r_2 = 0.3, 0.2, 0.1$ and 0.05. These values are chosen so as to be smaller than the value of MSD for the $EF1$ mechanism. It was found that for $r_2 = 0.05$, the DE algorithm could not converge to a feasible solution. The optimized mechanisms for $r_2 = 0.3, 0.2$ and 0.1 are shown in Table 1 (mechanisms 2–4). Mechanisms 5–7 (Table 2) represent the ‘ $EF2$ ’ mechanisms, with w=0.5,1.5 and 2.0 respectively. Representative plots of φ versus θ are shown in Figs. 7–9, for mechanisms 1, 4 and 7 respectively. In these figures, the corner points of the rectangular path are indicated. Severe slope discontinuities are visible at two of the corner points, in Fig. 7 ($P2$ and $P4$). In each plot, the point of maximum slope discontinuity is indicated by a cross ($\times$) symbol. Since the synthesized mechanisms trace the specified path points exactly, generated and specified path points coincide. The error between generated and specified path segments between adjacent path points would depend on the interpolation scheme used to vary the control parameter ‘ φ ’ in between the specified path points. This issue needs to be investigated further, and is not within the scope of the present work.

From the comparison of the ‘ $EF1$ ’ and ‘ $EF1$ with constraint on MSD ’ mechanisms, (mechanisms1 and 2–4), it is observed that $\Delta\varphi$ increases, as the constraint is imposed on MSD and as r_2 decreases. The values of $\Delta\varphi$ are seen to be 2.8705^0 , 5.3572^0 , 10.1585^0 and 16.2663^0 respectively, for mechanisms 1, 2, 3 and 4. It is observed that the constraint imposed on MSD is almost satisfied with equality, by mechanisms 2-4. It can be concluded that for the specified path, and the chosen variable ranges, there exists an inverse relation between $\Delta\varphi$ and MSD . This approach is seen to have a limitation in that, below a particular value of r_2 , the optimization algorithm may not converge to a feasible solution.

From the comparison of the‘ $EF1$ ’ and ‘ $EF2$ ’ mechanisms (mechanisms 1 and 5–7), it is observed that MSD decreases and $\Delta\varphi$ increases, as the weight factor ‘ w ’ is increased. The values of $\Delta\varphi$ are seen to be 2.8705^0 , 3.0711^0 , 17.3778^0 and 17.4179^0 respectively, for mechanisms 1, 5, 6 and 7, whereas the values of MSD are seen to be 0.4769, 0.3529, 0.0361 and 0.0359 respectively. The results indicate that increasing ‘ w ’ beyond 2.0 is unlikely to further reduce *MSD*. It is apparent that the slope continuity characteristic of the control parameter can be improved by increasing the value of ‘ w ’, up to a certain extent.

The plots of φ v/s θ shown in Figs. 7–9 indicate that the slope continuity is better for mechanisms 4 (Fig. 8) and 7 (Fig. 9), than for mechanism 1 (Fig. 7). The slope continuity of mechanism 7 is seen to be the best among the three mechanisms. These visual observations are consistent with the MSD values of these mechanisms, presented in Tables 1 and 2. It should be noted that the y-axis scales are different in Figs. 7–9.

Table 2. Optimized '$EF2$' mechanisms.

Design Variables	**EF2**		
	(5)	**(6)**	**(7)**
	$w = 0.5$	$w = 1.5$	$w = 2.0$
X_A	2.8340	-3.0321	-3.0202
Y_A	3.7666	-3.7758	3.7760
X_E	4.0000	1.3088	1.3498
Y_E	3.8578	-1.5356	1.6103
L_2	3.5240	0.8142	0.8146
L_3	4.7575	2.8718	2.9725
L_4	4.6060	4.8813	4.8748
ρ	348.2323^0	327.8063^0	33.0310^0
L_1	0.7933	0.8142	0.8129
L_5	4.7594	4.8836	4.8766
OF	0.2301	0.3575	0.3758
$\Delta\varphi(rad)$	0.0536	0.3033	0.3040
MSD	**0.3529**	**0.0361**	**0.0359**

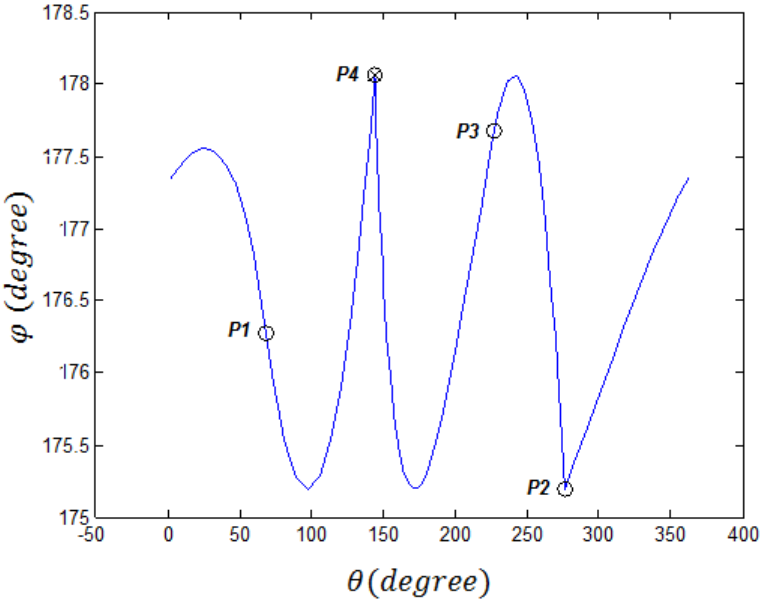

Fig. 7. Plot of φ v/s θ for mechanism 1 $(EF1)$.

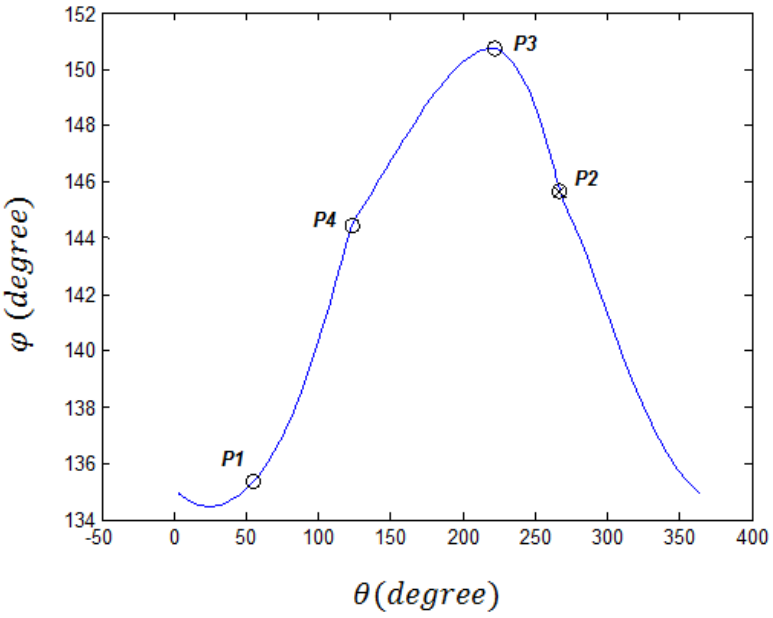

Fig. 8. Plot of φ v/s θ for mechanism 4 ($EF1$ with constraint on MSD, $r_2 = 0.1$).

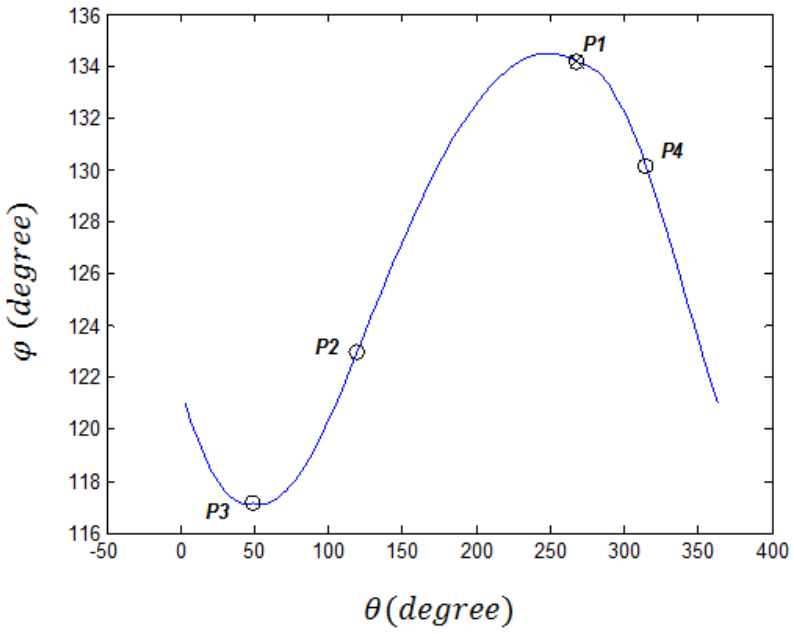

Fig. 9. Plot of φ v/s θ for mechanism 7 ($EF2$, w=2.0).

Discussion:

Results show that the two approaches developed in this work can be used to synthesize the proposed adjustable four-bar mechanism for path generation, so as to possess better slope continuity characteristics of the control parameter. The approach based on imposition of an upper limit on the value of MSD provides the designer with a direct control over MSD. However, it is not guaranteed that the optimization algorithm will converge to a feasible mechanism, when a constraint is imposed on MSD. The approach based on the use of the error function $EF2$ can be used to improve the slope continuity of the control parameter, at the cost of the net change in the control parameter. This approach does not suffer from the limitation of the first approach, and provides the designer with an indirect control over MSD.

8. CONCLUSION

In this work, optimum synthesis of a path generating adjustable four-bar mechanism, with an alternate single parameter adjustment, is presented. Two approaches are proposed to tackle the problem of slope discontinuity of the control parameter with respect to the input variable. Towards this, a 'maximum slope discontinuity' term (MSD) is defined. The first approach is based on imposing an upper limit on MSD, during the process of optimization. The second approach is based on using a newly proposed error function, which contains the 'maximum slope discontinuity' term. The Differential Evolution algorithm is used for optimization. A new scheme, called as the 'modified Chebyshev spacing' is used to discretize the specified path. Results are presented for an example problem.

Results show that the approach based on the imposition of a constraint on MSD ensures that the synthesized mechanism has an improved slope continuity characteristic, thus providing the designer with a direct control over the value of MSD. However, the optimization algorithm may not converge to a feasible mechanism. The approach based on the use of the new error function $EF2$ does not suffer from this limitation. It can be used to improve the slope continuity of the control parameter, which is accompanied by an increase in the total change in the control parameter. It provides the designer with an indirect control over MSD.

Both the proposed approaches have two distinct advantages over the 'modified path' approach proposed in [9]. Firstly, the designer can have a control over the degree of slope discontinuity of the control parameter. Secondly, and more importantly, the mechanism is synthesized for the specified path, rather than for a modified path as in the case of the 'modified path' approach.

REFERENCES

1. Starns, G. and Flugrad, D.R., "Five-bar path generation synthesis by continuation methods," *Transactions of ASME Journal of Mechanical Design*, Vol. 115, No. 4, pp. 988–994, 1993.
2. Nokleby, S.B. and Podhorodeski, R P., "Optimization based synthesis of Grashof geared five-bar mechanisms," *Transactions of ASME Journal of Mechanical Design*, Vol. 123, No. 4, pp. 529–534, 2001.
3. Mundo, D., Gatti, G. and Dooner, D.B., "Optimized five-bar linkages with non-circular gears for exact path generation," *Mechanism and Machine Theory*, Vol. 44, No. 4, pp. 751–760, 2009.
4. Zhou, H. and Ting, K.L, "Path generation with singularity avoidance for five-bar slider-crank parallel manipulators," *Mechanism and Machine Theory*, Vol. 40, No. 3, pp. 371–384, 2005.
5. Kay, F.J. and Haws, R.E., "Adjustable mechanisms for exact path generation," *Transactions of ASME Journal of Engineering for Industry*, Vol. 97, No. 2, pp. 702–707, 1975.

6. Zhou, H. and Ting, K.L, "Adjustable slider-crank linkages for multiple path generation," *Mechanism and Machine Theory*, Vol. 37, No. 5, pp. 499–509, 2002.
7. Singh, Y.P. and Kohli, D., "Synthesis of cam-link mechanisms for exact path generation," *Mechanism and Machine Theory*, Vol. 16, No. 4, pp. 447–457, 1981.
8. Zhou, H., "Synthesis of adjustable function generation linkages using the optimal pivot adjustment," *Mechanism and Machine Theory*, Vol. 44, No. 5, pp. 983–990, 2009.
9. Zhou, H., "Dimensional synthesis of adjustable path generation linkages using the optimal slider adjustment," *Mechanism and Machine Theory*, Vol. 44, No. 10, pp. 1866–1876, 2009.
10. Lin, W., "A GA–DE hybrid evolutionary algorithm for path synthesis of four-bar linkage," *Mechanism and Machine Theory*, Vol. 45, No. 8, pp. 1096–1107, 2010.
11. Cabrera, J.A., Ortiz, A., Nadal, F. and Castillo, J.J., "An evolutionary algorithm for path synthesis of mechanisms," *Mechanism and Machine Theory*, Vol. 46, No. 2, pp. 127-141, 2011.
12. Ghosh, A. and Mallik, A.K., *Theory of Mechanisms and Machines*, 2nd ed., Affiliated East-West Press, New Delhi, India, 1988.
13. Price, K.V., Storn, R.M. and Lampinen, J.A., *Differential Evolution. A Practical Approach to Global Optimization*, 1st ed., Springer, 2005.
14. Acharyya, S. and Mandal, M., "Performance of EAs for four-bar linkage synthesis," *Mechanism and Machine Theory*, Vol. 44, No. 9, pp. 1784 – 1794, 2009.